

Protein dynamics and electron transfer: Electronic decoherence and non-Condon effects

Spiros S. Skourtis*[†], Ilya A. Balabin[‡], Tsutomu Kawatsu[‡], and David N. Beratan*[†]

*Department of Physics, University of Cyprus, P.O. Box 20537, Nicosia 1678, Cyprus; and [‡]Departments of Chemistry and Biochemistry, Duke University, Durham, NC 27708

Edited by Harry B. Gray, California Institute of Technology, Pasadena, CA, and approved January 27, 2005 (received for review December 6, 2004)

We compute the autocorrelation function of the donor-acceptor tunneling matrix element $\langle T_{DA}(t)T_{DA}(0) \rangle$ for six Ru-azurin derivatives. Comparison of this decay time to the decay time of the time-dependent Franck–Condon factor {computed by Rossky and coworkers [Lockwood, D. M., Cheng, Y.-K. & Rossky, P. J. (2001) *Chem. Phys. Lett.* 345, 159–165]} reveals the extent to which non-Condon effects influence the electron-transfer rate. $\langle T_{DA}(t)T_{DA}(0) \rangle$ is studied as a function of donor-acceptor distance, tunneling pathway structure, tunneling energy, and temperature to explore the structural and dynamical origins of non-Condon effects. For azurin, the correlation function is remarkably insensitive to tunneling pathway structure. The decay time is only slightly shorter than it is for solvent-mediated electron transfer in small organic molecules and originates, largely, from fluctuations of valence angles rather than bond lengths.

correlation functions | Franck–Condon breakdown | dephasing | coupling pathways | redox reactions

The interplay among nuclear motion and electronic dynamics is the subject of increasing focus in the field of electron transfer (ET) processes (1–8). Recent research has focused on the effects of bridge nuclear motion on ET, with chemical, biological, and electronic device applications (see refs. 9–11 for reviews). Early theoretical analysis indicates that tunneling matrix element modulation by bridge dynamics can alter the free energy dependence of ET reaction rates by causing the Born–Oppenheimer (12) and Franck–Condon approximations to fail (13–15). More recently, theoretical studies explored ET kinetics in systems with fluctuating donor–acceptor matrix elements (16–24). Bridge motion can cause large and rapid donor–acceptor matrix element fluctuations, affecting the tunneling pathway structure and the interferences among pathways (25–37). The coupling matrix element fluctuations may have large contributions from solvent-polarization fluctuations (23), and these fluctuations facilitate electronically forbidden and gated ET (38–47). Finally, bridge–nuclear relaxation creates inelastic tunneling pathway channels (11, 20, 24, 47–49) that can change the mechanism of ET from superexchange to resonant tunneling to sequential hopping (11, 41–44, 50–62) and can lead to breakdown of the Born–Oppenheimer approximation (63, 64).

The goal of this work is to characterize tunneling matrix element fluctuations in azurin and, in particular, to examine their influence on the ET rate and on the validity of the Franck–Condon approximation. Franck–Condon breakdown can reduce the ET rate in the case of activationless ET reactions and enhance the rate for activated ET (18). ET in Ru-modified azurin is nearly activationless, and the protein is often approximated as being a rigid medium for tunneling because the tunneling pathways traverse a β sheet. In this work, we compute the effects of tunneling matrix element fluctuations on the rate as a function of distance, temperature, protein structural fluctuations, and intervening pathway structure. Further, we identify the types of motion that cause the coupling to fluctuate.

The general derivation of the nonadiabatic rate expression for fluctuating donor–acceptor matrix elements cannot assume the validity of the Franck–Condon separation. As explained below, the Franck–Condon approximation is only applicable when matrix element fluctuations are slower than the decay time of the thermally

weighted nuclear Franck–Condon overlap factor. This decay time, τ_{FC} , measures the escape time of the system from regions of Franck–Condon allowed transitions. τ_{FC} is roughly the time it takes for two nuclear wavepackets to lose overlap when they are initially placed at the crossing point between the donor and acceptor diabatic energy surfaces and each is allowed to move on a separate surface. $\tau_{FC} \approx \hbar/\sqrt{2\lambda K_B T}$, where λ is the total reorganization energy and T is the temperature (65, 66).

ET Rates and Correlation Functions

The argument above about the validity of the Franck–Condon approximation can be derived from a time-dependent formulation of the ET rate. In the vibronic state representation, the nonadiabatic rate is a thermally weighted sum of energy-conserving transitions between initial $|D; v, a\rangle$ and final $|A; w, b\rangle$ Born–Oppenheimer vibronic levels, i.e.,

$$k_{DA} = \frac{2\pi}{\hbar} \sum_v \sum_a P_{Dv} P_a \sum_w \sum_b |\langle D; v, a | \hat{T} | A; w, b \rangle|^2 \cdot \delta[E_D + \varepsilon_v + \varepsilon_a - (E_A + \varepsilon_w + \varepsilon_b)], \quad [1]$$

(1–7, 20, 24, 67), where $|D\rangle$ and $|A\rangle$ are the donor and acceptor electronic states, and $|v\rangle$ and $|w\rangle$ are vibrational levels associated with the donor and acceptor diabatic energy surfaces. These vibrations modulate the energies of $|D\rangle$ and $|A\rangle$ but not the tunneling barrier between them. $|a\rangle$ and $|b\rangle$ are vibrational levels associated with vibrations that modulate only the tunneling barrier (dominantly orientational modes for long-distance ET). The energies of $|D; v, a\rangle$ and $|A; w, b\rangle$ are $E_D + \varepsilon_v + \varepsilon_a$ and $E_A + \varepsilon_w + \varepsilon_b$, respectively, where E_D and E_A denote the minimum electronic state energies and ε_i denotes vibrational state energies. The thermal probability of the initial vibronic state $|D; v, a\rangle$ is taken to be the product $P_{Dv} P_a$ of the thermal probabilities of the vibrational levels $|v\rangle$ and $|a\rangle$ (consistent with the assumption that motions affecting the donor and acceptor energies are independent of those affecting the tunneling barrier). The scattering operator \hat{T} in Eq. 1 is given by

$$\hat{T} = \hat{V} \hat{G}^{\text{br}}(E_{\text{tun}}) \hat{V}, \quad [2]$$

where \hat{V} is the donor-bridge/acceptor-bridge electronic coupling operator and \hat{G}^{br} is the bridge electronic/vibronic Green's function. \hat{T} describes tunneling transitions between the electronic $|D\rangle$ and $|A\rangle$ states that are accompanied by transitions between bridge vibrational states, i.e., $\langle D; v, a | \hat{T} | A; w, b \rangle = \langle v | w \rangle \langle a | \hat{T}_{DA} | b \rangle$ where $\hat{T}_{DA} \equiv \langle D | \hat{T} | A \rangle$ is an operator in the space of bridge vibrational levels. This characteristic means that the tunneling electron can interact with the bridge vibrations (e.g., refs. 14, 20, 47, and 49).

This paper was submitted directly (Track II) to the PNAS office.

Abbreviations: ET, electron transfer; MD, molecular dynamics.

[†]To whom correspondence may be addressed. E-mail: skourtis@ucy.ac.cy or david.beratan@duke.edu.

© 2005 by The National Academy of Sciences of the USA

By using the Fourier representations of the δ -function in Eq. 1 (68), the nonadiabatic rate is

$$k_{DA} = \frac{1}{\hbar^2} \int_{-\infty}^{\infty} dt e^{i[E_D - E_A]t/\hbar} \langle \hat{T}_{DA}(t) \hat{T}_{AD}(0) \rangle_B \langle e^{i\hat{h}_D t/\hbar} e^{-i\hat{h}_A t/\hbar} \rangle_D, \quad [3]$$

where

$$\langle \hat{T}_{DA}(t) \hat{T}_{AD}(0) \rangle_B = \sum_a P_a \langle a | \hat{T}_{DA}(t) \hat{T}_{AD}(0) | a \rangle, \quad [4]$$

is the thermal correlation function of the tunneling operator in Eq. 2. $\hat{T}_{DA}(0) = \langle D | \hat{T} | A \rangle$ and $\hat{T}_{DA}(t) = e^{i\hat{h}_B t/\hbar} \hat{T}_{DA}(0) e^{-i\hat{h}_B t/\hbar}$, where $\hat{h}_B = \sum_a \epsilon_a |a\rangle\langle a|$ is the bridge vibrational Hamiltonian. The term

$$\langle e^{i\hat{h}_D t/\hbar} e^{-i\hat{h}_A t/\hbar} \rangle_D = \sum_v P_{Dv} \langle v | e^{i\hat{h}_D t/\hbar} e^{-i\hat{h}_A t/\hbar} | v \rangle, \quad [5]$$

is the thermally weighted time-dependent Franck–Condon factor ($\hat{h}_D = \sum_v \epsilon_v |v\rangle\langle v|$ and $\hat{h}_A = \sum_w \epsilon_w |w\rangle\langle w|$ are the vibrational Hamiltonians for the donor and acceptor energy surfaces).

Eq. 3 is a time-domain expression for the rate, equivalent to the energy-domain expression in Eq. 1 (its Fourier transform). It provides a time-dependent view of the Condon approximation breakdown. The time integral in Eq. 3 is the Fourier transform of the product of two decaying functions, $C_{T_{DA}}(t) = \langle \hat{T}_{DA}(t) \hat{T}_{AD}(0) \rangle_B$ and $C_{FC}(t) = \langle e^{i\hat{h}_D t/\hbar} e^{-i\hat{h}_A t/\hbar} \rangle_D$, evaluated at the D – A energy gap frequency. To recover the standard expression for the Franck–Condon rate, we replace $C_{T_{DA}}(t)$ in Eq. 3 by $C_{T_{DA}}(0) = \langle \hat{T}_{DA}^2(0) \rangle$ and factor it out of the integral, i.e.,

$$k_{DA} \approx \frac{1}{\hbar^2} \langle \hat{T}_{DA}^2(0) \rangle \int_{-\infty}^{\infty} dt e^{i[E_D - E_A]t/\hbar} \langle e^{i\hat{h}_D t/\hbar} e^{-i\hat{h}_A t/\hbar} \rangle_D. \quad [6]$$

A necessary condition for the validity of this approximation is that $C_{FC}(t)$ decays much more rapidly than $C_{T_{DA}}(t)$. The time integral in Eq. 3 is equal to the convolution integral $(2\pi)^{-1} \int_{-\infty}^{\infty} d\omega \tilde{C}_{T_{DA}}([E_D - E_A]/\hbar - \omega) \times \tilde{C}_{FC}(\omega)$ of the Fourier transforms of $C_{FC}(t)$ and $C_{T_{DA}}(t)$. If $C_{FC}(t)$ decays much faster than $C_{T_{DA}}(t)$, then the width of $\tilde{C}_{FC}(\omega)$ is much greater than the width of $\tilde{C}_{T_{DA}}([E_D - E_A]/\hbar - \omega)$ (assuming roughly Lorentzian or Gaussian envelopes for both functions). Therefore, in the frequency region around $\omega_{DA} = [E_D - E_A]/\hbar$, where $\tilde{C}_{T_{DA}}([E_D - E_A]/\hbar - \omega)$ is nonzero, $\tilde{C}_{FC}(\omega)$ is a slowly varying function. Substituting $\tilde{C}_{FC}(\omega) \approx \tilde{C}_{FC}(\omega_{DA}) + (\omega - \omega_{DA}) \times d\tilde{C}_{FC}(\omega_{DA})/d\omega$ in the convolution integral, and keeping only $\tilde{C}_{FC}(\omega_{DA})$, gives $\tilde{C}_{FC}(\omega_{DA}) \times (2\pi)^{-1} \int_{-\infty}^{\infty} d\omega' \tilde{C}_{T_{DA}}(\omega')$ (where $\omega' = \omega_{DA} - \omega$). This zeroth-order expression is equivalent to Eq. 6, because $(2\pi)^{-1} \int_{-\infty}^{\infty} d\omega' \tilde{C}_{T_{DA}}(\omega') = C_{T_{DA}}(t=0) = \langle \hat{T}_{DA}^2(0) \rangle$, and $\tilde{C}_{FC}(\omega_{DA})$ is the time integral of Eq. 6. Corrections to the Franck–Condon rate can be derived by retaining higher-order terms in the Taylor expansion of $\tilde{C}_{FC}(\omega)$. Non-Condon corrections generally depend on $E_D - E_A$, in addition to the decay times of $C_{FC}(t)$ and $C_{T_{DA}}(t)$ (17–19, 22, 24), because the energy gap determines a third time scale in Eq. 3, the oscillation period of the exponential.

The advantage of the time-domain description (Eq. 3) is that the decay times of $C_{FC}(t)$ and $C_{T_{DA}}(t)$ can be associated readily with structural fluctuations of the molecule and its solvent, by using molecular dynamics (MD) simulations and semiclassical approximations of the correlation functions. In the classical limit for bridge motion, the $\hat{T}_{DA}(t)$ matrix elements averaged over bridge vibrational states (Eq. 4) are replaced by a superexchange matrix element that is modulated by the classical bridge trajectories $R(t)$ [i.e., $T_{DA}(t) = T_{DA}[R(t)]$]. In this case, the averages in Eqs. 4 and 5 become averages over classical trajectories.

Correlation Functions in Azurin

To our knowledge, the only computation of the short-time decay of $C_{FC}(t)$ for a biological ET system was carried out for azurin by Lockwood *et al.* (69). The decay was computed by using the frozen Gaussian approximation for the nuclear wavepackets (70, 71). The multidimensional nuclear wave functions were approximated as products of atom-centered Gaussian wavepackets of constant widths moving along classical trajectories (obtained by MD simulations). In this case, $C_{FC}(t)$ is the thermal average of the time-dependent overlap $\langle \psi^D(t) | \psi^A(t) \rangle$ between an initial nuclear wavepacket propagated with the electron in the donor state and the same wavepacket propagated with the electron in the acceptor state. The time it takes to lose overlap is τ_{FC} . In this semiclassical approach, the rate in Eq. 3 is

$$k_{DA}^{FC} \approx \frac{1}{\hbar^2} \int_{-\infty}^{\infty} dt e^{i[E_D - E_A]t/\hbar} \langle T_{DA}(t) T_{DA}(0) \rangle_T \langle \langle \psi^D(t) | \psi^A(t) \rangle \rangle_T, \quad [7]$$

where $T_{DA}(t)$ is the superexchange matrix element evaluated along classical nuclear trajectories, and $\langle \rangle_T$ denotes the classical thermal average. Lockwood *et al.* (69) reported $\tau_{FC} = 3$ – 4 fsec with contributions from both solvent and protein matrix relaxation. Their value is consistent with the estimate $\tau_{FC} \approx \hbar/\sqrt{2\lambda K_B T} \approx 3$ fsec, with $\lambda \approx 1$ eV (1 eV = 1.602×10^{-19} J) at room temperature. Although τ_{FC} is not the only time scale associated with the thermally weighted Franck–Condon factor (65, 66), it seems that, at least in the case of azurin, it is the shortest time scale.

$T_{DA}(t)$ fluctuations have been studied for many ET systems using MD simulations and quantum chemical semiempirical calculations (20, 25, 27–37). In most cases, large fluctuations in T_{DA} were observed, sometimes on time scales as short as tens of femtoseconds. A measure of the fluctuations of $T_{DA}(t)$ is the coherence parameter, defined as $R_{\text{coh}} = \langle T_{DA}^2 \rangle / \langle T_{DA} \rangle^2$ (32). For a flexible bridge with multiple interfering tunneling pathways R_{coh} approaches zero. The coherence parameter is the infinite time limit of the normalized autocorrelation function, $R_{\text{coh}} = \lim_{t \rightarrow \infty} C_{T_{DA}}(t) / C_{T_{DA}}(0)$ (in the classical limit for the nuclear motion). The coherence parameter does not contain information about how fast coherence is lost as a result of the fluctuations in the matrix element. This information is contained in the decay time of $C_{T_{DA}}(t)$, τ_{coh} . Analysis of the spin–boson model with an exponentially decaying $C_{T_{DA}}(t)$ ($C_{T_{DA}}(t) \propto \exp[-t/\tau_{\text{coh}}]$) has shown a complex dependence of the non-Condon rate on τ_{coh} (18). Matrix element fluctuations may enhance or reduce the ET rate (with respect to its static, infinite τ_{coh} value), depending on the relative magnitudes of the reorganization energy and the driving force (18).

Recently, a perturbative theory was developed (24) to calculate non-Condon corrections to the ET rate. The theory is based on the Taylor expansion of $\tilde{C}_{FC}(\omega)$ described in the previous section. It is equivalent to an expansion of the rate in terms of R_{coh} and τ_{coh} , and it gives a lowest-order correction to the classical Marcus rate equal to

$$k^{(2)} = k^{(0)} \times (\hbar^2 \tau_{\text{coh}}^{-2}) (1 - R_{\text{coh}}) 2((\lambda + \Delta E^0)^2 - 2\lambda K_B T) / (4\lambda K_B T)^2, \quad [8]$$

where $k^{(0)}$ is the Marcus rate, λ the reorganization energy, and ΔE^0 is the driving force of the reaction. $k^{(2)}$ also depends on $(\tau_{FC})^2$, as seen by substituting $\sqrt{2\lambda K_B T} \approx \hbar/\tau_{FC}$ in Eq. 8. R_{coh} and τ_{coh} were computed from MD/semiempirical simulations of a C-clamp donor–acceptor molecule in different solvents (37). $C_{T_{DA}}(t)$ showed a decay time of $\tau_{\text{coh}} \approx 0.1$ psec and a coherence parameter close to zero. These values gave a negligible non-Condon correction to the rate (0.04%) based on Eq. 8.

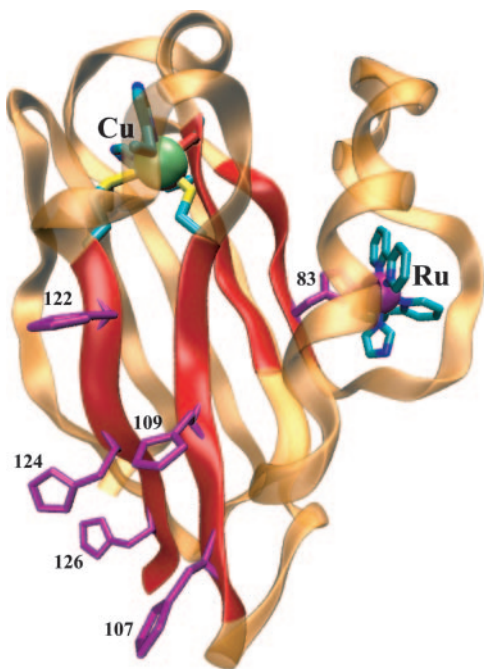


Fig. 1. Structures of the Ru-modified WT azurin 1BEX and its mutants, H83G Q107H, H83G M109H, H83G K122H, H83G T124H, and H83G T126H, used in the calculations of the T_{DA} correlation functions.

To our knowledge, this C-clamp molecule analysis is the only computation of $C_{T_{DA}}(t)$ for an ET system. Because Franck–Condon breakdown depends on the relative decay times of $C_{T_{DA}}(t)$ and $C_{FC}(t)$, it is important to explore $C_{T_{DA}}(t)$ for a biological ET system like azurin, where there is a wealth of experimental information on the rates (72–76), as well as prior analysis of $C_{FC}(t)$ (69). Here, we compute $C_{T_{DA}}(t)$ for the Ru-modified azurin with Protein Data Bank ID code 1BEX (77) and some of its mutants. We use MD simulations and extended-Hückel electronic structure calculations to compute $C_{T_{DA}}(t)$. Given the femtosecond-time-scale decay of $C_{FC}(t)$ (69), we focus on the short time decay of $C_{T_{DA}}(t)$ and interpret this decay in terms of protein structure and dynamics. Fig. 1 shows the structure of azurin and positions of the histidine residues linked to the Ru-bipyridine complex in the wild type (WT) and the derivatives as follows: H83G Q107H, H83G M109H, H83G K122H, H83G T124H, and H83G T126H. The donor–acceptor pairs were chosen to study $C_{T_{DA}}(t)$ as a function of the following: (i) average (MD-based) donor–acceptor distance (metal-to-metal), T122H (14 Å), WT (17 Å), M109H (19 Å), T124H (22 Å), Q107H (25 Å), and T126H (25 Å); (ii) distance along the same covalent pathway, (T122H vs. T124H and T126H); and (iii) intervening medium structure (covalent, hydrogen-bonded, or mixed pathways) for approximately the same average donor–acceptor distance (Q107H and T126H). Further, for all donor–acceptor pairs, $C_{T_{DA}}(t)$ is computed for a range of tunneling energies to assess the sensitivity of the correlation function to D/A energetics.

By choosing donor–acceptor pairs with similar immediate environments, we aim to isolate the effects of bridge structure and dynamics on $C_{T_{DA}}(t)$. Further, because of the approximations contained in MD simulations and extended-Hückel calculations, we seek generic features of the correlation functions that are robust with respect to parameter choice (e.g., tunneling energy) and geometric constraints. Only the short-time dynamics of $C_{T_{DA}}(t)$ are explored because the initial decay of the Franck–Condon factor is very rapid.

MD Simulations. The simulated *Pseudomonas aeruginosa* azurin structures were based on the Protein Data Bank structure 1BEX

(77). Five other structures with different locations of the Ru-bipyridine complex were modeled by performing a H83G mutation and Q107H, M109H, K122H, T124H, or T126H mutations using the SYBYL molecular modeling package (Version 6.5, Tripos Associates, St. Louis). The Ru-bipyridine complex was added to each derivative by using the program VMD (www.ks.uiuc.edu/Research/vmd) and the 1BEX structure as a template. All structures were solvated in bulk TIP3 water, and Na^+ and Cl^- counterions were added to an ionic strength of 200 mM. The resulting structures included 18,267–19,420 atoms and had dimensions of $\approx 55 \times 57 \times 53 \text{ \AA}^3$.

The structures underwent energy minimization for 500 steps with harmonic constraints imposed on the protein backbone and Ru-bipyridine complex, followed by equilibration for 200 psec with the same constraints and 1 nsec without constraints at 310 K. Simulations were performed on up to 300 processors at the Duke University Center for Computational Science, Engineering and Medicine cluster (www.csem.duke.edu) and on the Biophysics Cluster at the University of Cyprus, by using the programs CHARMM (78) and NAMD (www.ks.uiuc.edu/Research/namd) with the CHARMM force field (79), isothermal–isobaric (NpT) ensemble, periodic boundary conditions, a Langevin thermostat, and full electrostatics particle-mesh Ewald calculations (80). The force-field parameters for the copper center were taken from ref. 81, and the parameters for the Ru-bipyridine complex were taken from ref. 27. Protein conformation samples for the effective coupling calculations were obtained by performing three series of MD simulations (5,000 conformations saved every 1, 10, and 100 fsec, respectively) at 310 K for each derivative.

To explore how protein structural motion affects the correlation function decay time, additional MD simulations were performed for the WT 1BEX as follows: (i) Simulations with no constraints at 100, 30, 10, and 3 K (preceded by a 1-nsec-long equilibration at these temperatures); (ii) simulations at 310 K with SHAKE constraints on all bonds to suppress bond-length fluctuations [the program CHARMM (78) was used for this simulation, because implementation of the SHAKE algorithm in NAMD2 is limited to bonds with hydrogen atoms]; and (iii) simulations at 310 K with SHAKE constraints on all bonds with hydrogen atoms and all valence angle force constants (including Urey–Bradley terms) scaled up by a factor of 1,000 to suppress fluctuations of both bond lengths and valence angles (these simulations were performed with integration time step of 0.1 fsec).

T_{DA} Calculations. In the superexchange regime, the effective tunneling coupling is given by refs. 82 and 83

$$T_{DA}(E) = \sum_{ij \neq D,A} [E\bar{S} - \bar{H}]_{Di}^{(d)} [(E - \bar{H})^{-1}]_{ij}^{(b)} [E\bar{S} - \bar{H}]_{jA}^{(a)}, \quad [9]$$

where \bar{S} and \bar{H} are the orbital overlap and Hamiltonian matrices of the donor [index (d)], bridge [index (b)], and acceptor [index (a)], respectively. The calculations were performed by using Slater-type valence orbitals and an extended-Hückel Hamiltonian. Calculations at this level are rapid and provide reasonable qualitative estimates of the effective tunneling matrix elements in proteins and small molecules (32, 35, 83–90)

The calculations were performed by using code based on the program FORTICON8 (91), ITPACK2C routines (92), and parameters for the extended-Hückel Hamiltonian and the Slater orbitals based on density functional calculations (93). To describe the extent of mixing the initial with final states onto the bridge, the effective electronic coupling was renormalized with the method described in refs. 35, 90, and 94 as follows:

$$T_{DA}^{\text{norm}}(E_{\text{tun}}) = \frac{T_{DA}(E_{\text{tun}})}{\sqrt{1 - \partial T_{DD}(E_{\text{tun}}) / \partial E_{\text{tun}}} \sqrt{1 - \partial T_{AA}(E_{\text{tun}}) / \partial E_{\text{tun}}}}. \quad [10]$$

Table 1. Distance and medium dependence at $T = 310$ K and $E_{\text{tun}} = -10.8$ eV

| Structure | R_{coh} | $\varepsilon_{R_{\text{coh}}}$ | τ_{coh} , fs | $\varepsilon_{\tau_{\text{coh}}}$, fs | $\langle R_{DA} \rangle$, Å |
|-----------|------------------|--------------------------------|--------------------------|--|------------------------------|
| K122H | 0.04 | 0.06 | 26.7 | 9.7 | 13.8 |
| WT 83H | 0.12 | 0.08 | 34.9 | 15.2 | 17.3 |
| M109H | 0.03 | 0.07 | 55.9 | 32.3 | 19.1 |
| T124H | 0.11 | 0.09 | 27.5 | 10.2 | 21.9 |
| Q107H | 0.07 | 0.06 | 20.3 | 6.4 | 24.8 |
| T126H | 0.01 | 0.02 | 26.6 | 9.8 | 25.1 |

3 shows these values for the WT at 310 K and different constraints imposed on the protein. The first row of the table reports values obtained for unconstrained MD. The second row data were computed with constraints on all bond lengths (*vide supra*). The third row shows the values computed with constraints on lengths of bonds with hydrogen atoms and all valence angle force constants scaled up by a factor of 1,000.

The tables are representative of the results we obtained for different 5,000-fsec trajectories. The mutants T122H, T124H, and T126H lie along the same covalent pathway, whereas Q107H and T126H have approximately the same donor–acceptor distance but different intervening pathways (Fig. 1). Table 1 shows that the decay of $\langle T_{DA}(t)T_{DA}(0) \rangle$ for all structures is of the order of a few tens of femtoseconds, and the coherence parameter $\langle T_{DA} \rangle^2 / \langle T_{DA}^2 \rangle$ is of the order of 0.1 or less. Therefore, both R_{coh} and τ_{coh} are robust, changing little with donor–acceptor distance and intervening medium. Table 2 shows that R_{coh} and τ_{coh} change little with temperature. An increase in R_{coh} is observed only at 30 K and lower temperatures (not probed in experiments), whereas τ_{coh} does not depend on temperature within the statistical error.

Table 3 summarizes how constraints on protein structural flexibility influence R_{coh} and τ_{coh} . Use of different constraints, along with the temperature dependence, provides a strategy to identify specific kinds of protein motion that control these two parameters. The $T_{DA}(t)$ time series show the major fluctuations on the time scale of tens of femtoseconds. Much smaller amplitude fluctuations of the femtosecond time scale are superimposed on the major fluctuations. These two time scales correspond to valence angle vibrations and covalent bond vibrations, respectively. MD does not accurately describe the time dependence of bond vibrations, but it does give the correct order of magnitude for the rms deviations of bond lengths. Therefore, we expect that the magnitudes of matrix element fluctuations caused by bond vibrations, as predicted by MD, are of the right order of magnitude. The first kind of constraints used in our simulations was the SHAKE constraints on all bond lengths (including the donor and acceptor units). In the $T_{DA}(t)$ time dependence, these constraints eliminate the weak (femtosecond time scale) fluctuations but have a negligible effect on the strong (tens of femtoseconds) fluctuations. Accordingly, as shown in Table 3, neither R_{coh} nor τ_{coh} is significantly affected by the SHAKE constraints, indicating that these parameters are not sensitive to covalent bond vibrations. The other kind of constraints included the SHAKE constraints on lengths of all bonds with hydrogen atoms, combined with scaling up all force constants for

Table 2. Temperature dependence for WT at $E_{\text{tun}} = -10.8$ eV

| Temp., K | R_{coh} | $\varepsilon_{R_{\text{coh}}}$ | τ_{coh} , fs | $\varepsilon_{\tau_{\text{coh}}}$, fs |
|----------|------------------|--------------------------------|--------------------------|--|
| 310 | 0.12 | 0.08 | 34.9 | 15.2 |
| 100 | 0.21 | 0.12 | 52.5 | 28.8 |
| 30 | 0.60 | 0.10 | 44.1 | 25.3 |
| 10 | 0.66 | 0.12 | 43.0 | 19.8 |
| 3 | 0.86 | 0.10 | 30.8 | 14.4 |

Temp., temperature.

Table 3. Constraint dependence for WT at $T = 310$ K and $E_{\text{tun}} = -10.8$ eV

| Structural constraints | R_{coh} | $\varepsilon_{R_{\text{coh}}}$ | τ_{coh} , fs | $\varepsilon_{\tau_{\text{coh}}}$, fs |
|---|------------------|--------------------------------|--------------------------|--|
| None | 0.12 | 0.08 | 34.9 | 15.2 |
| SHAKE (all bonds) | 0.08 | 0.11 | 39.1 | 21.1 |
| SHAKE (bonds with hydrogens and all valence angles) | 0.06 | 0.14 | 68.5 | 44.5 |

valence angles. Suppressing both the fastest bond vibrations and all valence angle vibrations, these constraints visibly increase the time scale of the major $T_{DA}(t)$ fluctuations, consistently increasing τ_{coh} by almost 80% (Table 3). Importantly, the 1,000-fold increase in the valence angle force constants has a similar effect on angle fluctuations as a 1,000-fold decrease in temperature, i.e., cooling the system down to ≈ 0.3 K. This result explains why no significant increase in τ_{coh} was observed in the simulations at low temperatures: even at 3 K, angle fluctuations were large enough to cause dephasing. In addition to the direct effect on dephasing, valence angle fluctuations also drive dihedral angle fluctuations that, in turn, modulate the lengths of hydrogen bonds, thereby affecting the electronic interference among the dominant ET pathways and T_{DA} (32). Indeed, we observed a decrease of $>30\%$ in dihedral angle fluctuations caused by imposing the above constraints. However, these constraints have no significant effect on R_{coh} , suggesting that the latter is controlled not only by valence angle fluctuations but also by dihedral angle fluctuations, which dominate the slower motion of the protein structure.

Finally, we do not find a significant dependence of R_{coh} and τ_{coh} on the electron tunneling energy for relevant ET tunneling energies in azurin. A large effect of the tunneling energy on τ_{coh} was observed only when the tunneling energy was artificially brought into resonance with bridge-centered eigenstates. In this case, τ_{coh} dropped, and coherence was lost within 5 fsec. This situation is not expected to be relevant to the Ru-modified derivatives examined here, but recent experiments with highly oxidizing ET reagents in proteins may access this regime (100, 101). Moreover, near-resonant ET may be relevant to DNA ET (8), as well as to unsaturated organic ET systems with low donor(acceptor)-bridge energy gaps (41, 42).

Fast coherence loss in azurin arises from T_{DA} fluctuations on the time scale of tens of femtoseconds. The time scale for coherence loss is long compared with the Franck–Condon time of 3–4 fsec for azurin computed by Lockwood *et al.* (69) (the latter is in agreement with the estimate $\tau_{FC} \approx \hbar / \sqrt{2\lambda k_B T} = 3$ fsec for $\lambda \approx 1$ eV at room temperature). Therefore, we expect the Franck–Condon approximation to Eq. 6 to be accurate for single-step tunneling in azurin.

Interestingly, the values of R_{coh} and τ_{coh} in azurin are not very different from those computed (37) for ET in a much smaller C-clamp-shaped donor–acceptor molecule. In the C-clamps, fluctuations in the superexchange interaction through solvent presumably lead to the decoherence. The time scale of this decoherence is within an order of magnitude of the electronic decoherence time computed here for the Ru-modified azurins. By using Eq. 8 for azurin with an average $\tau_{\text{coh}} \approx 30$ fsec, $\lambda \approx 1$ eV, and $\Delta E^0 \approx -\lambda$, gives a correction of 0.8% of the Marcus rate. As in the case of ET in C-clamped molecules, for ET in azurin non-Condon effects are not significant.

The type of non-Condon effects considered here are relevant to ET reactions through avoided crossings. If ET involves an electronic transition at a conical intersection (102) (as may be the case in excited-state ET), non-Condon effects are significant. In this situation, the Born–Oppenheimer approximation is not valid at the avoided crossing, and corrections to the superexchange expression for the tunneling matrix element must be considered (63).

Conclusions

Simulations of the tunneling matrix element autocorrelation function for Ru-modified WT azurin and several of its mutants show that the decay of $\langle T_{DA}(t)T_{DA}(0) \rangle$ is rapid, with a time constant of a few tens of femtoseconds. The coherence parameter $R_{\text{coh}} = \langle T_{DA} \rangle^2 / \langle T_{DA}^2 \rangle$ is of the order of 0.1 or less. This finding means that azurin is a fluctuating medium for tunneling with multiple interfering tunneling pathways. Within the statistical errors of our analysis, we cannot ascertain any significant dependence of R_{coh} and τ_{coh} on the donor–acceptor distance or intervening medium structure or any sensitivity to the presence or absence of chemical bond vibrations. Importantly, decoherence occurs on the time scale of valence angle fluctuations, indicating the central role of valence angle fluctuations in T_{DA} dephasing. All computed τ_{coh} values are an order of magnitude longer than the decay time of the thermally weighted

Franck–Condon factor τ_{FC} , computed by Lockwood *et al.* (69) to be 3–4 fsec. Therefore, non-Condon effects are insignificant for the case of azurin in the deep tunneling regime. As tunneling energies approach the charge injection limit, the Condon approximation will likely fail.

The methodology described in this work is suited for the study of dynamics–function relationships for ET reactions. An interesting question that should be addressed, by using this methodology, is whether non-Condon effects and dephasing characteristics of proteins vary with their secondary (and tertiary) structures.

S.S.S. was supported by University of Cyprus Research Grant “Repair of UV-damaged DNA by DNA Photolyase: Insights from Molecular Dynamics and Electron Transfer Calculations.” D.N.B. was supported by National Institutes of Health Grant GM-048043 and by the Duke Center for Computational Science, Engineering and Medicine.

- Marcus, R. A. & Sutin, N. (1985) *Biochim. Biophys. Acta* **811**, 265–322.
- Kuznetsov, A. M. (1995) *Charge Transfer in Physics, Chemistry and Biology* (Gordon & Breach, Amsterdam).
- Jortner, J. & Ratner, M., eds. (1997) *Molecular Electronics* (Blackwell Scientific, Oxford).
- Kuznetsov, A. M. & Ulstrup, J. (1999) *Electron Transfer in Chemistry and Biology* (Wiley, Chichester, U.K.).
- Jortner, J. & Bixon, M., eds. (1999) *Electron Transfer: From Isolated Molecules to Biomolecules*, Advances in Chemical Physics (Wiley, New York), Vols. 106–107.
- May, V. & Kühn, O. (2000) *Charge and Energy Transfer Dynamics in Molecular Systems* (Wiley–VCH, Berlin).
- Balzani, V., Piotrowiak, P., Rodgers, M. A. J., Mattay, J., Astruc, D., Gray, H. B., Fukuzumi, S., Mallouk, T. E., Haas, Y., de Silva, A. P. & Gould, I. R., eds. (2001) *Electron Transfer in Chemistry* (Wiley–VCH, Weinheim, Germany), Vols. I–V.
- Schuster, G. B., ed. (2004) *Topics in Current Chemistry: Long-Range Charge Transfer in DNA* (Springer, Berlin), Vols. 236–237.
- Newton, M. D. (2001) in *Electron Transfer in Chemistry*, ed. Balzani, V. (Wiley–VCH, Weinheim, Germany), Vol. 1, pp. 3–63.
- Skourtis, S. S. & Beratan, D. N. (2001) in *Electron Transfer in Chemistry*, ed. Balzani, V. (Wiley–VCH, Weinheim, Germany), Vol. 1, pp. 109–125.
- Nitzan, A. (2001) *Annu. Rev. Phys. Chem.* **52**, 681–750.
- Beratan, D. N. & Hopfield, J. J. (1984) *J. Chem. Phys.* **81**, 5753–5759.
- Onuchic, J. N., Beratan, D. N. & Hopfield, J. J. (1986) *J. Phys. Chem.* **90**, 3707–3721.
- Onuchic, J. N. & Da Gama, A. A. S. (1986) *Theor. Chim. Acta* **69**, 89–100.
- Mikkelsen, K. V., Ulstrup, J. & Zakaraya, M. G. (1989) *J. Am. Chem. Soc.* **111**, 1315–1319.
- Kuznetsov, A. M., Vigdorovich, M. D. & Ulstrup, J. (1993) *Chem. Phys.* **176**, 539–554.
- Goldstein, R. F., Franzen, S. & Bialek, W. (1993) *J. Phys. Chem.* **97**, 11168–11174.
- Tang, J. (1993) *J. Chem. Phys.* **98**, 6263–6266.
- Goychuk, I. A., Petrov, E. G. & May, V. (1995) *J. Chem. Phys.* **103**, 4937–4944.
- Medvedev, E. S. & Stuchebrukhov, A. A. (1997) *J. Chem. Phys.* **107**, 3821–3831.
- Liao, J. L. & Voth, G. A. (2002) *J. Chem. Phys.* **116**, 9174–9187.
- Bixon, M. & Jortner, J. (2003) *Russian J. Electrochem.* **39**, 5–10.
- Milischuk, A. & Matyushov, D. (2003) *J. Chem. Phys.* **118**, 5596–5606.
- Troisi, A., Nitzan, A. & Ratner, M. A. (2003) *J. Chem. Phys.* **119**, 5782–5788.
- Wolfgang, J., Risser, S. M., Priyadarshy, S. & Beratan, D. N. (1997) *J. Phys. Chem. B* **101**, 2986–2991.
- Daizadeh, I., Medvedev, E. S. & Stuchebrukhov, A. A. (1997) *Proc. Natl. Acad. Sci. USA* **94**, 3703–3708.
- Ungar, L. W., Newton, M. D. & Voth, G. A. (1999) *J. Phys. Chem. B* **103**, 7367–7382.
- Miller, N. E., Wander, M. C. & Cave, R. J. (1999) *J. Phys. Chem. A* **103**, 1084–1093.
- Castner, E. W., Kennedy, D. & Cave, R. J. (2000) *J. Phys. Chem. A* **104**, 2869–2885.
- Xie, Q., Archontis, G. & Skourtis, S. S. (1999) *Chem. Phys. Lett.* **312**, 237–246.
- Skourtis, S. S., Xie, Q. & Archontis, G. (2001) *J. Chem. Phys.* **115**, 9444–9462.
- Balabin, I. A. & Onuchic, J. N. (2000) *Science* **290**, 114–117.
- Newton, M. D. (2000) *Int. J. Quantum Chem.* **77**, 255–263.
- Troisi, A. & Orlandi, G. (2002) *J. Phys. Chem. B* **106**, 2093–2101.
- Kawatsu, T., Kakitani, T. & Yamato, T. (2002) *J. Phys. Chem. B* **106**, 11356–11366.
- Zimmt, M. B. & Waldeck, D. H. (2003) *J. Phys. Chem. A* **107**, 3580–3597.
- Troisi, A., Ratner, M. A. & Zimmt, M. B. (2004) *J. Am. Chem. Soc.* **126**, 2215–2224.
- Reimers, J. R., Hush, N. S., Sammeth, D. M. & Callis, P. R. (1990) *Chem. Phys. Lett.* **169**, 622–626.
- Reimers, J. R. & Hush, N. S. (1990) *Chem. Phys.* **146**, 105–114.
- Yip, W. T., Levy, D. H., Kobetic, R. & Piotrowiak, P. (1999) *J. Phys. Chem. A* **103**, 10–20.
- Davis, W. B., Svec, W. A., Ratner, M. A. & Wasielewski, M. R. (1998) *Nature* **396**, 60–63.
- Davis, W. B., Ratner, M. A. & Wasielewski, M. R. (2001) *J. Am. Chem. Soc.* **123**, 7877–7886.
- Schlag, E. W., Sheu, S.-Y., Yang, D.-Y., Selzle, H. L. & Lin, S. H. (2000) *Proc. Natl. Acad. Sci. USA* **97**, 1068–1072.
- Schlag, E. W., Yang, D.-Y., Sheu, S.-Y., Selzle, H. L., Lin, S. H. & Rentzepis, P. M. (2000) *Proc. Natl. Acad. Sci. USA* **97**, 9849–9854.
- Jones, G. A., Paddon-Row, M. N., Carpenter, B. K. & Piotrowiak, P. (2002) *J. Phys. Chem. A* **106**, 5011–5021.
- Troisi, A., Ratner, M. A. & Nitzan, A. (2003) *J. Chem. Phys.* **118**, 6072–6082.
- Skourtis, S. S., Waldeck, D. H. & Beratan, D. N. (2004) *J. Phys. Chem. B* **108**, 15511–15518.
- Nitzan, A., Jortner, J., Wilkie, J., Burin, A. L. & Ratner, M. A. (2000) *J. Phys. Chem. B* **104**, 5661–5665.
- Galperin, M., Nitzan, A. & Benjamin, I. (2002) *J. Phys. Chem. A* **106**, 10790–10796.
- Friis, E. P., Kharkats, Y. I., Kuznetsov, A. M. & Ulstrup, J. (1998) *J. Phys. Chem. A* **102**, 7851–7859.
- Kuznetsov, A. M. & Ulstrup, J. (2002) *J. Chem. Phys.* **116**, 2149–2165.
- Davis, W. B., Wasielewski, M. R., Ratner, M. A., Mujica, V. & Nitzan, A. (1997) *J. Phys. Chem. A* **101**, 6158–6164.
- Hu, Y. & Mukamel, S. (1989) *J. Chem. Phys.* **91**, 6973–6988.
- Skourtis, S. S. & Mukamel, S. (1995) *Chem. Phys.* **197**, 367–388.
- Kühn, I., Rupasov, V. & Mukamel, S. (1996) *J. Chem. Phys.* **104**, 5821–5833.
- Okada, A., Chernyak, V. & Mukamel, S. (1998) *J. Phys. Chem. A* **102**, 1241–1251.
- Kimura, A. & Kakitani, T. (1998) *Chem. Phys. Lett.* **298**, 241–249.
- Sumi, H. & Kakitani, T. (2001) *J. Phys. Chem. B* **105**, 9603–9622.
- Berlin, Y. A., Burin, A. L. & Ratner, M. A. (2000) *J. Phys. Chem. A* **104**, 443–445.
- Petrov, E. G., Shevchenko, Y. V., Teslenko, V. I. & May, V. (2001) *J. Chem. Phys.* **115**, 7107–7122.
- Bixon, M. & Jortner, J. (2002) *Chem. Phys.* **281**, 393–408.
- Renger, T. & Marcus, R. A. (2003) *J. Phys. Chem. A* **107**, 8404–8419.
- Skourtis, S. S. (2003) *Chem. Phys. Lett.* **372**, 224–231.
- Medvedev, E. S. & Stuchebrukhov, A. A. (2004) *Chem. Phys.* **296**, 181–192.
- Onuchic, J. N. & Wolynes, P. G. (1988) *J. Phys. Chem.* **92**, 6495–6503.
- Bialek, W., Bruno, W. J., Joseph, J. & Onuchic, J. N. (1989) *Photosynth. Res.* **22**, 15–27.
- Levich, V. G. & Dogonadze, R. R. (1959) *Dokl. Acad. Nauk SSSR* **124**, 123–126.
- Lax, M. (1952) *J. Chem. Phys.* **20**, 1752–1760.
- Lockwood, D. N., Cheng, Y.-K. & Rossky, P. J. (2001) *Chem. Phys. Lett.* **345**, 159–165.
- Neria, E. & Nitzan, A. (1993) *J. Chem. Phys.* **99**, 1109–1123.
- Prezhdo, O. V. & Rossky, P. J. (1997) *J. Chem. Phys.* **107**, 5863–5878.
- Gray, H. B. & Winkler, J. R. (2003) *Q. Rev. Biophys.* **36**, 341–372.
- Gray, H. B. & Winkler, J. R. (1996) *Annu. Rev. Biochem.* **65**, 537–561.
- Langen, R., Chang, I.-J., Germanas, J. P., Richards, J. H., Winkler, J. R. & Gray, H. B. (1995) *Science* **268**, 1733–1735.
- Onuchic, J. N., Beratan, D. N., Winkler, J. R. & Gray, H. B. (1992) *Annu. Rev. Biophys. Biomol. Struct.* **21**, 249–377.
- Regan, J. J., Di Bilio, A. J., Langen, R., Skov, L. K., Winkler, J. R., Gray, H. B. & Onuchic, J. N. (1995) *Chem. Biol.* **2**, 489–496.
- Faham, S., Day, M. W., Connick, W. B., Crane, B. R., Di Bilio, A. J., Schaefer, W. P., Rees, D. C. & Gray, H. B. (1999) *Acta Crystallogr. D* **55**, 379–385.
- Brooks, B., Brucoleri, R., Olafson, B., States, D., Swaminathan, S. & Karplus, M. (1983) *J. Comput. Chem.* **4**, 187–217.
- Mackerell, A., Bashford, D., Bellott, M., Dunbrack, R., Evanseck, J., Field, M., Fischer, S., Gao, J., Guo, H., Ha, S., *et al.* (1998) *J. Phys. Chem. B* **102**, 3586–3616.
- Darden, T., York, D. & Pedersen, L. (1997) *J. Chem. Phys.* **98**, 10089–10092.
- Ungar, L. W., Scherer, N. F. & Voth, G. A. (1997) *Biophys. J.* **72**, 5–17.
- Priyadarshy, S., Skourtis, S. S., Risser, S. M. & Beratan, D. N. (1996) *J. Chem. Phys.* **104**, 9473–9481.
- Balabin, I. A. & Onuchic, J. N. (1998) *J. Phys. Chem.* **102**, 7497–7505.
- Siddarth, P. & Marcus, R. A. (1990) *J. Phys. Chem.* **94**, 8430–8434.
- Siddarth, P. & Marcus, R. A. (1993) *J. Phys. Chem.* **97**, 13078–13082.
- Tan, M. L., Balabin, I. A. & Onuchic, J. N. (2003) *Biophys. J.* **86**, 1813–1819.
- Balabin, I. A. & Onuchic, J. N. (1996) *J. Phys. Chem.* **100**, 11573–11580.
- Daizadeh, I., Gehlen, J. N. & Stuchebrukhov, A. A. (1997) *J. Chem. Phys.* **106**, 5658–5666.
- Kawatsu, T., Kakitani, T. & Yamato, T. (2000) *Inorg. Chim. Acta* **300–302**, 862–868.
- Kawatsu, T., Kakitani, T. & Yamato, T. (2002) *J. Phys. Chem. B* **106**, 5068–5074.
- Howell, J., Rossi, A., Wallace, D., Haraki, K. & Hoffmann, R. (1977) *FORTICON 8 (Extended-Hückel Program)* (Quantum Chemistry Program Exchange, Indiana Univ., Bloomington, IN), QCPE 11, No. 344.
- Kincaid, D. R., Respass, J. R., Young, D. M. & Grimes, R. G. (1999) *ITPACK 2C: A Fortran Package for Solving Large Sparse Linear Systems by Adaptive Accelerated Iterative Methods* (Univ. of Texas, Austin, TX).
- Vela, A. & Gázquez, J. L. (1988) *J. Phys. Chem.* **92**, 5688–5693.
- Katz, D. J. & Stuchebrukhov, A. A. (1998) *J. Chem. Phys.* **109**, 4960–4970.
- Penfold, K., Gerwith, A. & Solomon, E. I. (1985) *J. Am. Chem. Soc.* **107**, 4519–4529.
- Gerwith, A. & Solomon, E. I. (1988) *J. Am. Chem. Soc.* **110**, 3811–3819.
- Janke, W. (2002) in *Quantum Simulations of Complex Many-Body Systems: From Theory to Algorithms*, Lecture Notes, John von Neumann Institute for Computing Series, eds. Groten-dorst, J., Marx, D. & Muramatsu, A. (John von Neumann Institute for Computing, Jülich, Germany), Vol. 10, pp. 423–445.
- Frenkel, D. & Smit, B. (2002) *Understanding Molecular Simulation: From Algorithms to Applications* (Academic, San Diego).
- Flyvbjerg, H. & Petersen, H. G. (1989) *J. Chem. Phys.* **91**, 461–466.
- Miller, J. E., Di Bilio, A. J., Wehbi, W. A., Green, M. T., Museth, A. K., Richards, J. H., Winkler, J. R. & Gray, H. B. (2004) *Biochim. Biophys. Acta* **1655**, 59–63.
- Di Bilio, A. J., Crane, B. R., Wehbi, W. A., Kiser, C. N., Abu-Omar, M. M., Carlos, R. M., Richards, J. H., Winkler, J. R. & Gray, H. B. (2001) *J. Am. Chem. Soc.* **123**, 3181–3182.
- Klessinger, M. & Michl, J. (1995) *Excited States and Photo-Chemistry of Organic Molecules* (Wiley, New York).